Environmental Science & Technology

pubs.acs.org/est Article

Impacts of Ship Emissions on Air Quality in Southern China: Opportunistic Insights from the Abrupt Emission Changes in Early 2020

Xu Feng, Yaping Ma, Haipeng Lin, Tzung-May Fu,* Yan Zhang, Xiaolin Wang, Aoxing Zhang, Yupeng Yuan, Zimin Han, Jingbo Mao, Dakang Wang, Lei Zhu, Yujie Wu, Ying Li, and Xin Yang

Cite This: https://doi.org/10.1021/acs.est.3c04155 Read Online

ABSTRACT: In early 2020, two unique events perturbed ship emissions of pollutants around Southern China, proffering insights into the impacts of ship emissions on regional air quality: the decline of ship activities due to COVID-19 and the global enforcement of low-sulfur (<0.5%) fuel oil for ships. In January and February 2020, estimated ship emissions of NO_x, SO_2, and primary $PM_{2.5}$ over Southern China dropped by 19, 71, and 58%, respectively, relative to the same period in 2019. The decline of ship NO_x emissions was mostly over the coastal waters and inland waterways of Southern China due to reduced ship activities. The decline of ship SO_2 and primary $PM_{2.5}$ emissions was most pronounced outside the Chinese Domestic Emission Control Area due to the switch to low-sulfur fuel oil there. Ship emission reductions in early 2020 drove 16 to 18% decreases in surface NO_2 levels but 3.8 to 4.9% increases in surface ozone over Southern China. We estimated that ship emissions contributed 40% of surface NO_2 concentrations over Guangdong in winter. Our results indicated that future abatements of ship emissions should be implemented synergistically with reductions of land-borne anthropogenic emissions of nonmethane volatile organic compounds to effectively alleviate regional ozone pollution.

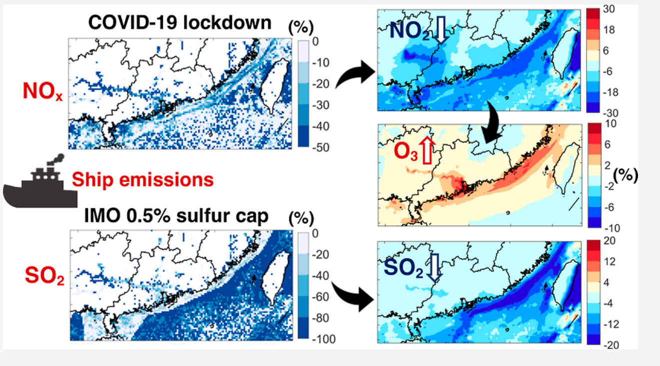

KEYWORDS: *ship emissions, COVID-19 pandemic, low-sulfur fuel oil, air quality*

1. INTRODUCTION

The coastal waters and inland waterways of Southern China are among the busiest areas for ship activities in the world. In 2020, the three major ports (Shenzhen, Guangzhou, and Hong Kong) in the Pearl River Delta (PRD) area of Southern China handled a total container throughput of 68 million twenty-foot equivalent units (TEUs), accounting for 8.9% of the global port container traffic.[1,2] The inland waterway throughput along the Pearl River in 2018 was 7.0 million TEUs, making up 24% of China's annual throughput of inland ports.[3] Furthermore, the number of registered motorized fishing boats in Guangdong province exceeded 54,000, 12% of China's fishing fleet in 2019.[4] As a result, ship emissions constitute an important source of air pollutants in Southern China, particularly given China's recent efforts to reduce land-borne anthropogenic pollutant emissions.[5−7] In 2019, ship emissions were responsible for 35, 28, and 35% of Hong Kong's estimated total anthropogenic emissions of NO_x ($NO_x = NO + NO_2$), SO_2, and primary $PM_{2.5}$, respectively.[8] Early observations showed that prior to recent abatement of land-borne emissions, ship emissions contributed 5 to 18% of the surface $PM_{2.5}$ concentrations in the PRD between 2009 and 2015.[9−11] However, the current impact of ship emissions on air quality in Southern China is unclear, partly due to the difficulty in discerning the impacts of ship emissions in the presence of land-borne pollutants.

In January and February 2020, two events caused abrupt changes in ship emissions of pollutants over the inland and coastal waters of Southern China, providing a unique opportunity to assess the impacts of ship emissions on air quality in the region. The first event was the worldwide curtailment of human activity levels due to coronavirus disease-2019 (COVID-19). Many studies have shown how the lockdown measures adopted by Chinese cities to contain the spread of COVID-19 led to sharp decreases in land-borne anthropogenic pollutant emissions and changes in urban air quality.[12−19] During the nationwide lockdown period in early

Received: June 1, 2023
Revised: September 30, 2023
Accepted: October 3, 2023

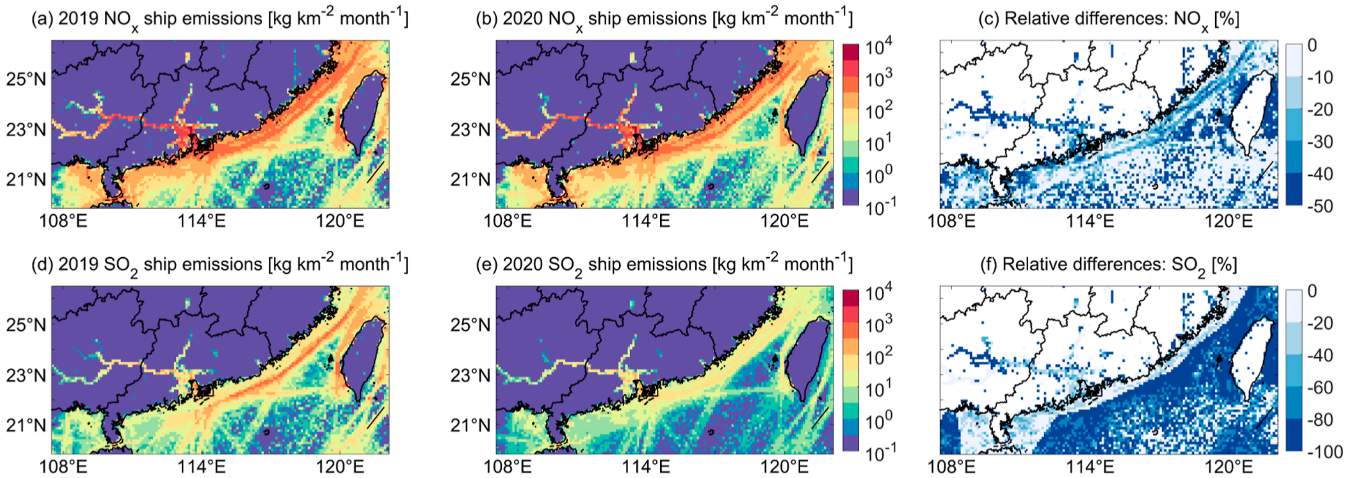

Figure 1. Spatial distributions of monthly mean ship emissions of (a,b) NO_x and (d,e) SO_2 during January and February of 2019 (left column) and 2020 (center column). Also shown are the percent changes of monthly mean ship emissions of (c) NO_x and (f) SO_2 in early 2020 relative to those in early 2019.

2020, the national mean urban concentrations of surface $PM_{2.5}$, NO_2, and SO_2 were 14, 16, and 12% lower than the concentrations during the same period in 2019, respectively.[18] In contrast, the national mean urban surface ozone concentrations were 9% higher during the lockdown period in 2020 compared to the same period in 2019, reflecting the nonlinear response of ozone photochemistry to its precursors.[18] Several studies have investigated how COVID-19 restrictions led to declined ship activities and emissions around the Yangtze River Delta and Eastern China.[20,21] However, the changes in ship emissions due to the COVID-19 crisis and their impacts on regional air quality in Southern China have not been quantified.

The second event that affected ship emissions was the International Maritime Organization (IMO)'s mandate of low-sulfur content (<0.5%) in ship fuel oil, which became effective worldwide on January 1, 2020.[22] The sulfur contents of the fuel oil are proportional to the emission factors of SO_2 and $PM_{2.5}$ from ships.[23,24] Since 2019, China has enforced the use of low-sulfur (<0.5%) fuel oil (LSFO) for vessels operating within the Chinese Domestic Emission Control Area (CDECA),[25] which included the inland waterways of the Yangtze and Pearl Rivers and a 12 nautical mile width zone along the Chinese coastline. Previous studies estimated that the use of LSFO within the CDECA would moderately lower the surface SO_2 and $PM_{2.5}$ concentrations over the PRD area by approximately 10 and 3%, respectively,[26,27] but those assessments were based on land-borne and ship emissions prior to the year 2015. The abrupt changes in ship emissions in early 2020 provide an opportunity to evaluate the effectiveness of the CDECA under present-day land-borne and ship emissions as well as the potential benefits of further reducing pollutant emissions within and outside the CDECA.

In this work, we quantified the changes in land-borne and ship emissions of pollutants over Southern China during early 2020 as a result of the decline of human activities associated with COVID-19 and the IMO's global enforcement of LSFO. We used a regional air quality model to conduct sensitivity simulations and assessed the impacts of ship emissions on present-day air quality in Southern China, with the goal of informing future ship emission policies for the betterment of air quality in this region.

2. METHODS

2.1. Anthropogenic Pollutant Emissions over Southern China during Early 2019 and 2020. We quantified the emissions of pollutants from ships in and around Southern China during January and February 2019 ("ShipEmis-2019" emissions) and 2020 ("ShipEmis-2020" emissions). Using the methods described in Fan et al.[23] and Yuan et al.,[28] we estimated the monthly ship emissions of SO_2, NO_x, CO, total nonmethane volatile organic compounds (NMVOCs), and primary $PM_{2.5}$ (including primary elemental carbon and organic aerosols, and primary noncarbonaceous aerosols) over East and South China Seas and the inland waterways of Southern China at a 0.1° resolution. Ship activity data were obtained from the dynamic monitoring of vessel tracks using the automatic identification system (AIS).[29] For 2019, we assumed that the sulfur contents of ship fuel oil were 0.5% within the CDECA and 2.7% elsewhere.[25,30] For 2020, we assumed that the sulfur contents of ship fuel oil were 0.5% everywhere, in accordance with the IMO's global LSFO mandate.[22] A recent observational study demonstrated that desulfurized heavy fuel oil is being used extensively around the PRD area to comply with the CDECA regulations.[31] There has not yet been a detailed investigation into the compliance of the IMO's LSFO mandate beyond the CDECA since 2020. However, the IMO's Global Integrated Shipping Information System[32] reported only 7 and 55 cases of nonavailability of compliant fuel oil in China and worldwide, respectively, throughout the year 2020. This small number of reports of ships encountering difficulty in obtaining compliant fuel provided evidence for the effective enforcement of the IMO's global LSFO policy. We assumed that the reduction of sulfur content in ship fuel oil proportionally decreased ship emissions of both SO_2 and primary $PM_{2.5}$,[23] supported by field observations.[26,33,34] We mapped the total NMVOC emissions to individual species using the emission profiles of the transportation sector (Table S1) in the Multiresolution Emission Inventory for China (MEIC) inventory.[35]

Land-based anthropogenic emissions in China were taken from the MEIC inventory,[36] which was originally developed for 2017 at a resolution of 0.25°. The inventory included emissions from power generation, industry, transportation (except ships), residential activities, and agriculture.[37] We first scaled the MEIC monthly emissions from 2017 to 2019 levels (referred to as "MEIC-2019") using national monthly statistics[13] (Table S2). We then estimated China's land-based anthropogenic emissions in January and February 2020 (referred to as "MEIC-2020") using monthly provincial and sectorial activity strength ratios relative to 2019.[13] Agricultural NH_3 emissions were held at their 2017 levels. Overall, the reduction in human activities due to COVID-19 lockdowns led to decreases of 11 and 38% (Figure S1 and Table S3) in land-based anthropogenic NO_x emissions over Southern China (domain shown in Figure 1) during January and February 2020, respectively, compared to the same months in 2019.

We further scaled the monthly provincial land-borne anthropogenic NO_x emissions in MEIC-2020 using the day-to-day variability of NO_x emissions in January and February 2020, which was derived from the TROPOspheric Monitoring Instrument (TROPOMI) tropospheric NO_2 column concentration retrievals.[12] This satellite-based constraint reflected the temporal variability of land-borne NO_x emissions affected by both the COVID-19 lockdowns and Chinese New Year. Daily NO_x emissions over Southern China gradually dropped in early January (Figure S2), reflecting the waning socioeconomic activities leading up to Chinese New Year (January 25, 2020). COVID-related lockdowns were observed in Hubei Province on January 23, 2020. Within a few days, most Chinese provinces had started enforcing restrictions on socioeconomic activities. Consequently, daily land-borne NO_x emissions were 9 to 37% below the monthly mean emissions during January 23 to February 9, 2020. In most Southern Chinese provinces, socioeconomic activities resumed after February 9, and daily land-borne NO_x emissions gradually returned to the monthly mean levels (Figure S2). For other land-borne anthropogenic pollutants, little information was available on their daily variation of emissions; we assumed that the daily emission rates between January 1 and 22, 2020 were the same as the monthly mean rates in January 2019 and that all emission reductions in January 2020 occurred between January 23 and 31, 2020. Daily emissions of land-borne anthropogenic pollutants (except NO_x) recovered to the monthly mean levels in February 2020.

2.2. WRF-GC Model Simulations. We used the WRF-GC model (v2.0, doi:10.5281/zenodo.4395258)[38−40] to simulate air quality over Southern China during January and February 2020. WRF-GC v2.0 is an online coupling of the Weather Research and Forecasting meteorological model (WRF, v3.9.1.1, https://github.com/NCAR/WRFV3/releases/tag/V3.9.1.1)[41,42] and the GEOS-Chem chemical transport model (v12.8.2, doi:10.5281/zenodo.3837666).[43] The model includes a detailed O_x-NO_x-VOC-halogen-aerosol chemical mechanism.[44−46] We used two nested model domains with horizontal resolutions of 27 and 9 km (Figure S3a), respectively, and 50 vertical layers. Initial and boundary conditions for meteorological variables were obtained from the National Centers for Environmental Prediction Final (NCEP FNL) dataset with a resolution of 1° (doi:10.5065/D6M043C6).[47] Chemical initial and boundary conditions were from a GEOS-Chem global simulation.[39] Details of other model configurations are summarized in Table S4. All simulations were conducted for January 1 and February 29, 2020; the first 4 days spun up the model. We divided the simulation into three periods for analyses: P1 (pre-lockdown period between January 5 and 22, 2020), P2 (lockdown period between January 23 and February 9, 2020), and P3 (post-lockdown period between February 10 and 29, 2020).

We conducted three sensitivity experiments with different combinations of ship- and land-borne emissions (Table 1).

Table 1. Configurations of WRF-GC Sensitivity Simulations

experiments	ALL19	ALL20	SHIP19
land-borne anthropogenic emissions	MEIC-2019	MEIC-2020	MEIC-2020
ship emissions	ShipEmis-2019	ShipEmis-2020	ShipEmis-2019
model version		WRF-GC v2.0	
simulation time		January 1 to February 29, 2020	
microphysics		Morrison two-moment[68]	
shortwave/longwave radiation		RRTMG[69]	
planetary boundary layer		MYNN2[70]	
land surface		Noah[71,72]	
surface layer		MM5 Monin-Obukhov[73]	
cumulus parameterization		New Tiedtke[74−76]	
aerosol-cloud-radiation interactions		on	

The "ALL20" experiment was driven by our estimated land-borne and ship emissions for early 2020 (MEIC-2020 and ShipEmis-2020 inventories), affected by the restricted human activities during COVID-19 and the IMO global regulations. The "ALL19" simulation was driven by ship- and land-borne emissions from 2019 (MEIC-2019 and ShipEmis-2019 inventories) to represent regional air quality without the impacts of the COVID-19 restrictions and the IMO global regulations. The "SHIP19" experiment used land-borne emissions for 2020 (MEIC-2020) and ship emissions from 2019 (ShipEmis-2019). The differences between the ALL20 and SHIP19 simulations demonstrated the impacts of ship emission changes in early 2020 on air quality (Section 3.3).

2.3. Surface and Satellite Observations of Air Quality over Southern China. We evaluated our simulations against hourly surface pollutant measurements over Southern China during January and February 2020, managed by the China National Environmental Monitoring Centre (http://www.cnemc.cn, last accessed: October 11, 2022) and the Hong Kong Environmental Protection Department (http://epd.gov.hk, last accessed: October 11, 2022). We applied a consistent data quality control protocol to all surface measurements,[48,49] excluded sites with less than 90% valid hourly measurements during January and February 2000 and averaged the hourly measurements onto the WRF-GC model grids for comparison with the simulations. Overall, we used hourly surface measurements from 85, 85, 86, and 77 sites for NO_2, SO_2, ozone, and $PM_{2.5}$, respectively, to evaluate our simulations.

We further analyzed the differences in tropospheric NO_2 column concentrations observed by the TROPOMI satellite instrument for the months of January and February between 2019 and 2020.[50] TROPOMI is a nadir-viewing multispectral spectrometer onboard the Sentinel-5 Precursor satellite, in a sun-synchronous orbit that crosses the equator at 13:30 local time.[51] The Level 3 monthly gridded products used in this analysis for 2019 and 2020 were derived by oversampling the Sentinel-5P TROPOMI Tropospheric NO_2 1-Orbit Level 2 data in Version 2 (S5P_L2__NO2____HiR)[52] at a 0.05° spatial resolution.[14,53,54] The retrieval algorithm for 2019 and 2020 data was based on the Differential Optical Absorption Spectroscopy (DOAS) technique and remained unchanged.[55]

https://doi.org/10.1021/acs.est.3c04155
Environ. Sci. Technol. XXXX, XXX, XXX−XXX

3. RESULTS

3.1. Abrupt Changes in Ship Emissions of Pollutants over Southern China in Early 2020. Figures 1 and S4 and Tables 2 and S3 compare pollutant emissions from ships and from land-borne anthropogenic sources over Southern China (domain shown in Figure 1: 107.5° E to 122.1° E, 19.8° N to 26.4° N) in January and February of 2019 and 2020. In January and February 2019, ship emissions of NO_x, SO_2, and primary $PM_{2.5}$ over Southern China were 189, 45, and 15 Gg, respectively. Ship emissions constituted 51, 28, and 15% of the total anthropogenic emissions of these pollutants over Southern China, respectively. In January and February 2020, ship emissions of NO_x dropped by 36 Gg (−19%) relative to the same period in 2019, which was comparable in magnitude to the 40 Gg reduction in land-borne anthropogenic NO_x emissions over Southern China. The reduction of ship NO_x emissions in early 2020 were mainly due to the reduced ship activities resulting from the COVID-19 pandemic and were most pronounced along the Chinese coastline and the Pearl River (Figure 1c). The switch to LSFO outside the CDECA had little impact on the NO_x emissions from ships. Our estimated 19% reduction in ship NO_x emissions in early 2020 relative to that in early 2019 was consistent with the reported 13% drop in container throughput at the three major ports in

Table 2. Ship Emissions of Pollutants over Southern China (Domain in Figure 1: 107.5° E to 122.1° E, 19.8° N to 26.4° N) in January and February of the Years 2019 and 2020

emissions (Gg $month^{-1}$)	NO_x	SO_2	CO	primary $PM_{2.5}$[a]	NMVOCs
Jan 2019	112	25	5.6	8.5	5.5
Feb 2019	77	20	3.8	6.5	3.7
Jan 2020	88	7.5	4.3	3.9	4.2
Feb 2020	65	5.6	3.2	2.5	3.1
relative changes (%)	$(Emis_{2020} - Emis_{2019})/Emis_{2019} \times 100\%$				
Jan	−22%	−70%	−23%	−54%	−24%
Feb	−16%	−72%	−16%	−62%	−16%

[a]Total primary $PM_{2.5}$ includes primary OC, EC, and noncarbonaceous aerosols.

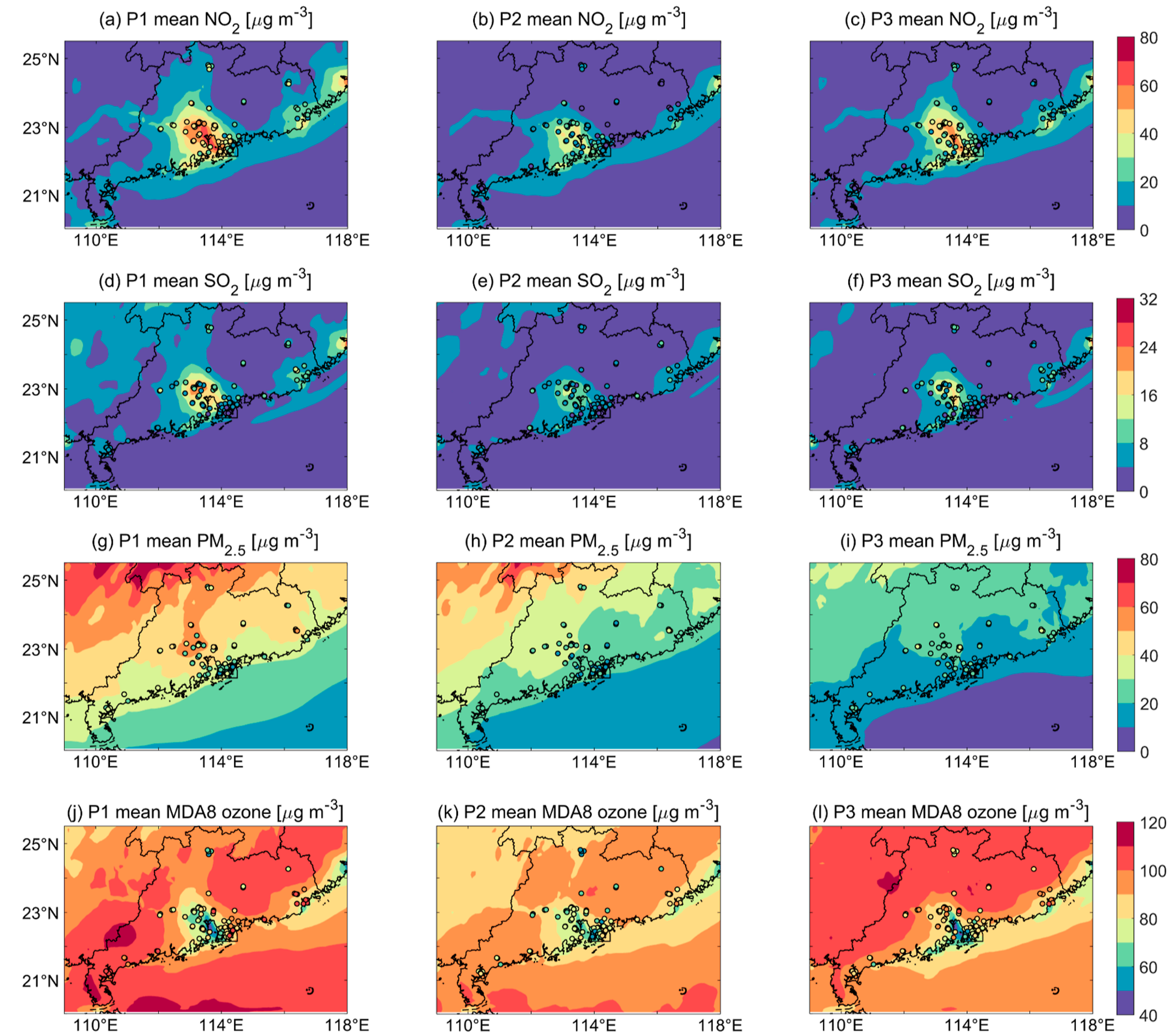

Figure 2. Comparisons of the observed (symbols) and simulated (ALL20 simulation, filled contours) surface concentrations of (a−c) NO_2, (d−f) SO_2, (g−i) $PM_{2.5}$, and (j−l) maximum daily 8 h average (MDA8) ozone during P1 (left column), P2 (center column), and P3 (right column) in early 2020.

https://doi.org/10.1021/acs.est.3c04155
Environ. Sci. Technol. XXXX, XXX, XXX−XXX

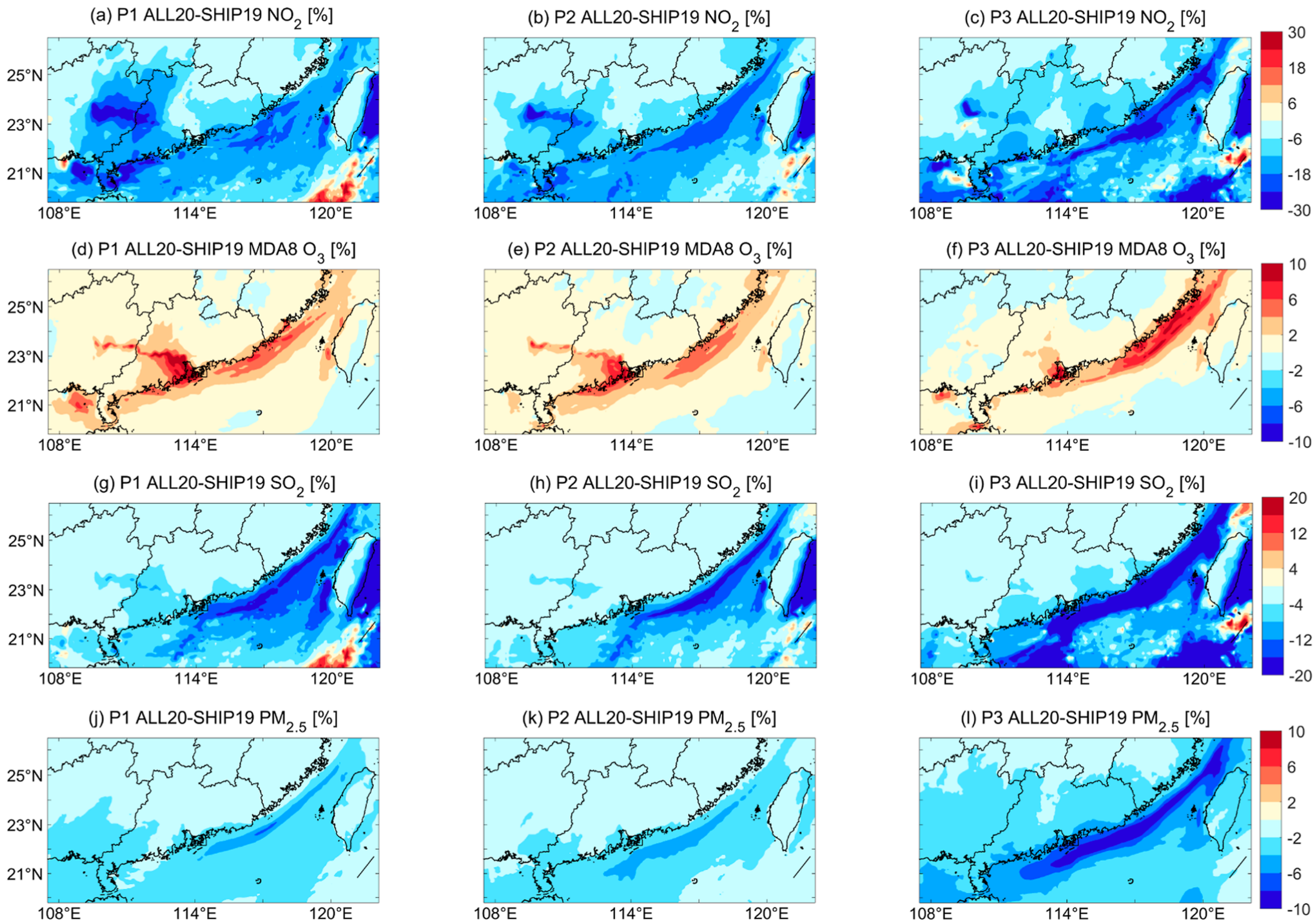

Figure 3. Simulated impacts on surface pollutant concentrations due to the changes of ship emissions during P1 (left column), P2 (center column), and P3 (right column) in early 2020: (a−c) NO_2, (d−f) MDA8 ozone, (g−i) SO_2, and (j−l) $PM_{2.5}$. For each pollutant, the impacts were quantified as the concentration differences between the ALL20 and SHIP19 experiments, relative to the concentrations in the ALL19 experiment.

the PRD area (Guangzhou, Shenzhen, and Hong Kong) during January and February 2020 relative to the same months in 2019 (Table S4).[56−58]

Ship emissions of SO_2 over Southern China dropped by 32 Gg (−71%) in January and February 2020, relative to the same period in 2019. This reduction was larger than the reductions of the land-borne emissions of SO_2 (24 Gg reduction, −21%). Primary $PM_{2.5}$ from ship emissions and land-borne emissions dropped by 8.6 Gg (−57%) and 12 Gg (−12%), respectively. Unlike the changes in ship NO_x emissions, the reductions of SO_2 and primary $PM_{2.5}$ emissions from ships in early 2020 were most pronounced outside the CDECA (areal average −85 and −80%, respectively) (Figures 1f and S5i), reflecting the impacts of the switch to LSFO outside the CDECA in January 2020. Within the CDECA, ship emissions of SO_2 and primary $PM_{2.5}$ were not affected by the IMO's new policy because of the existing LSFO regulations. However, ship emissions of both SO_2 and primary $PM_{2.5}$ still decreased by 20% as a result of the reduced ship activities in early 2020.

The spatial distributions and relative reductions of CO and NMVOC ship emissions in early 2020 were similar to those of NO_x ship emissions (see Figures S5). These emission changes were mainly affected by the COVID-19-related decline in ship activities. However, land-borne anthropogenic sources dominated the total anthropogenic emissions of these species over Southern China, rendering ship emissions relatively unimportant for the ambient concentrations of these air pollutants over this region during the winter (Figure S4).

3.2. Evaluation of Simulated Concentrations of Surface Air Pollutants over Southern China during Early 2020. Figure 2 and Table S5 compare our simulated (ALL20 simulation) surface concentrations of NO_2, SO_2, total $PM_{2.5}$ (including both primary and secondary $PM_{2.5}$) and maximum daily 8 h average (MDA8) ozone during the three stages of COVID-19 lockdown in 2020 against surface observations. During P2 and P3, the mean observed concentrations of NO_2 over Southern China were 20 ± 24 and 23 ± 14 $\mu g\ m^{-3}$, respectively. These values were 46 and 38% lower than the mean observed NO_2 concentrations before the lockdown (P1, 37 ± 18 $\mu g\ m^{-3}$), respectively. The largest observed decreases in NO_2 concentrations were over the megacities in the PRD area, reflecting the large decrement of land-borne NO_x emissions from traffic and industrial sources due to the COVID-19 lockdowns. The ALL20 simulation reproduced the observed NO_2 concentrations during P1 [34 ± 16 $\mu g\ m^{-3}$; normalized mean bias (NMB) against observations = −8.3%] and the relative decreases of NO_2 concentrations in P2 (20 ± 10 $\mu g\ m^{-3}$, NMB = −3.9%) and P3 (28 ± 13 $\mu g\ m^{-3}$, NMB = 18%). Given that the changes of NO_x emissions from ships and land-borne sources were comparable in magnitude in early 2020, and that the reductions of ship emissions of NO_2 were mostly along the inland waterways and coastline, our

https://doi.org/10.1021/acs.est.3c04155
Environ. Sci. Technol. XXXX, XXX, XXX−XXX

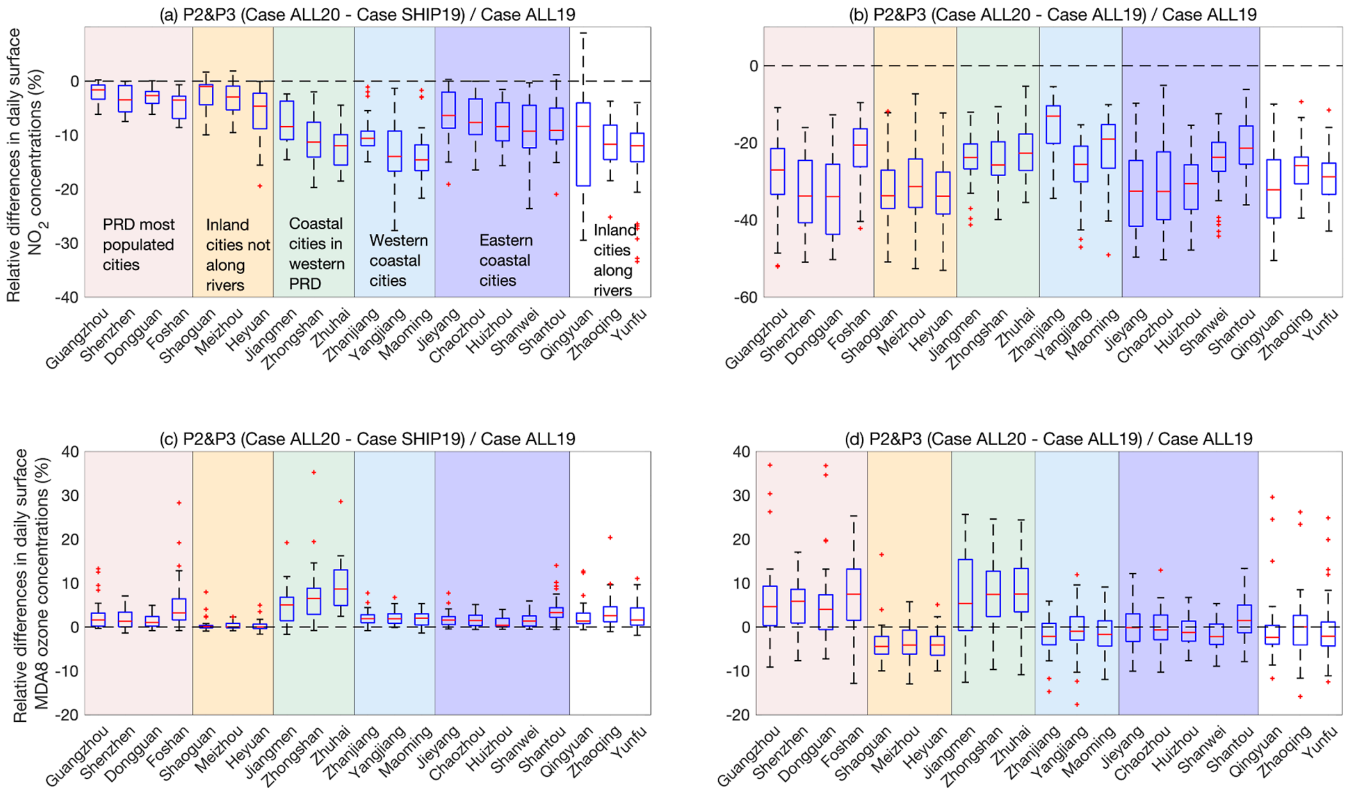

Figure 4. Box plots of the simulated impacts on surface pollutant concentrations over 21 Guangdong cities due to the changes in ship emissions (left column) and total anthropogenic emissions (right column) during P2 and P3 in 2020: (a,b) NO_2 and (c,d) MDA8 ozone. The impacts were quantified as the concentration differences between the ALL20 and SHIP19 experiments, relative to the concentrations in the ALL19 experiment. The cities are color-coded by their locations relative to the coast and inland waterways.

ability to simulate the observed changes in NO_x concentrations at the surface sites as shown in Figure 2 provided confidence in our estimated changes in ship emissions of NO_x.

Our simulated mean surface SO_2 and $PM_{2.5}$ concentrations were consistent with the surface measurements during P2 (SO_2: NMB = 5.0%; $PM_{2.5}$: NMB = 17%) and P3 (SO_2: NMB = 18%; $PM_{2.5}$: NMB = −19%). Our simulation overestimated the observed surface SO_2 (NMB = 39%) and $PM_{2.5}$ (NMB = 29%) concentrations during P1, potentially indicating an overestimation of the land-borne anthropogenic emissions of SO_2 from the MEIC-2020 and the transport of $PM_{2.5}$ from inland China.[59]

Surface ozone concentrations were also affected by abrupt emission changes over Southern China in early 2020. Mean observed surface MDA8 ozone concentrations at Southern Chinese sites during P1, P2, and P3 were 84 ± 15, 70 ± 10, and 82 ± 12 $\mu g\ m^{-3}$, respectively. Relative to P1, the observed MDA8 ozone concentrations decreased most significantly during P2 (−20%) over the minor cities in Northern and Eastern Guangdong, away from the PRD megacities and the coastline. Over the PRD megacities and along the coastline and the Pearl River, the observed decreases in MDA8 ozone were milder (−16%). These spatial differences in the response of ozone to precursor emission changes were consistent with previous analyses that showed, over Southern China in winter, that the photochemical production of surface ozone in the PRD megacities was in the "NO_x-saturated" or the "transitional" regimes. In these regimes, a decrease in local NO_x emissions would slow the removal of HO_x radicals or reduce the titration of ozone by NO, thereby increasing local ozone concentrations.[59,60] The photochemical production of surface ozone outside the PRD were more "NO_x-limited", such that reduction of local NO_x emission would slow the local photochemical production of ozone.[59,60]

The ALL20 simulation reproduced the mean observed surface MDA8 ozone concentrations over Southern China sites during P1 (85 ± 13 $\mu g\ m^{-3}$, NMB = 0.6%) and P3 (86 ± 11 $\mu g\ m^{-3}$, NMB = 4.6%), but the ALL20 simulation overestimated the observed MDA8 ozone during P2 (84 ± 8.1 $\mu g\ m^{-3}$, NMB = 19%). However, the simulated biases were mostly over rural areas in Northern and Eastern Guangdong. Over sites along the coast and the Pearl River, which were most affected by ship emissions, the simulated MDA8 ozone concentration during P2 was 82 ± 7.4 $\mu g\ m^{-3}$, which was more consistent with the observations in this area (76 ± 8.0 $\mu g\ m^{-3}$, NMB = 8%).

3.3. Impacts of Ship Emission Changes on Surface Air Quality over Southern China.

The evaluation above shows that the ALL20 simulation generally reproduced the observed surface concentrations of major air pollutants over Southern China and their relative temporal changes during three periods in early 2020. On that basis, we compared the differences in surface pollutant concentrations between the ALL20 and SHIP19 simulations relative to the ALL19 simulations (Figure 3) to quantify the impacts on regional air quality due to ship emission changes in early 2020. All simulations were for 2020, but the SHIP19 simulation was driven by ship emissions in 2019 (ShipEmis-2019 inventory).

Relative to ship emissions in 2019, ship emission changes in early 2020 led to 8.6 to 10% (0.8 to 1.2 $\mu g\ m^{-3}$) decreases in the mean simulated surface NO_2 concentrations over Southern China during the three periods in early 2020. The simulated decreases in surface NO_2 concentrations were most pronounced along the Pearl River in western Guangdong and over the coastal waters (16 to 18% decreases), since ship emissions constituted a major source of NO_x in this area affected by both marine and inland vessels (Figure 1). Over the East and South China seas, the recovery of ship activities to normal levels after the lockdown (P3) was slower than the recovery of land-borne anthropogenic activities.[21] As a result, there was a sustained decrease in NO_2 concentrations along the Pearl River and over the coastal waters during P3.

We aimed to assess whether our simulated impacts of ship emission changes on surface NO_2 in early 2020 were consistent with observations. However, no surface NO_2 measurements were available over the coastal waters of Southern China. Instead, we compared the differences in tropospheric NO_2 column concentrations observed by TROPOMI over the main ship lanes over Southern China in early 2019 and 2020 (Figure S6). We defined the main ship lanes as the 0.05° model grids where the NO_x emission from ships was higher than that from land-borne NO_x sources and where the NO_x emission from ships exceeded the 90th percentile of ship NO_x fluxes over Southern China (0.41 g m^{-2} $month^{-1}$). The TROPOMI-observed mean tropospheric NO_2 column concentration over the main ship lanes during January and February 2020 was 3.5 $\times 10^{15}$ molecules cm^{-2}, which was 13% lower than the mean observed tropospheric NO_2 concentration during the same period in 2019 (4.0 $\times 10^{15}$ molecules cm^{-2}, Figure S6b). This difference reflected the impacts of ship emission changes in early 2020, though part of the difference may be due to the discrepant meteorological conditions between early 2019 and early 2020. Our simulated reductions of mean tropospheric NO_2 column concentrations and surface NO_2 concentrations along the main ship lanes as a result of ship emission changes in early 2020 were both 18%, consistent with the TROPOMI observations.

Figure 4 depicts the simulated responses of daily mean NO_2 concentrations at the surface sites in 21 Guangdong cities (locations shown in Figure S3b) to changes in ship emissions alone and to the total changes in anthropogenic (ship- and land-borne) emissions during early 2020. Compared to the anthropogenic emissions at 2019 levels, the total changes in anthropogenic emissions during P2 and P3 led to a mean decrease of 26% in the simulated surface NO_2 concentrations in the 21 Guangdong cities (25th and 75th percentiles of relative changes were 22 to 31%, Figure 4b). We found that the minor cities along the coast and the inland waterways of Southern China were strongly affected by changes in ship emissions. The changes in total anthropogenic emissions caused a decrease of 10 to 42% in simulated surface NO_2 concentrations in these cities. The changes in ship emissions alone caused a decrease of 2 to 19% in simulated surface NO_2, comparable to the impacts of changes in land-borne emissions (Figure 4a,b). In contrast, in the four most populated cities in the PRD (Guangzhou, Shenzhen, Dongguan, and Foshan)[61] and in the minor inland cities not along the major waterways (Shaoguan, Meizhou, and Heyuan), most of the reduced NO_2 concentrations were driven by the decline of land-borne emissions. The changes in ship emissions alone led to only 1 to 9% decreases in the simulated surface NO_2 in these cities. On average, the estimated 19% reduction in ship NO_x emissions over Southern China in early 2020 drove an 8% mean decline in the simulated surface NO_2 concentrations over the 21 Guangdong cities. We thus estimated that ship NO_x emissions contributed to approximately 40% of surface NO_2 concentrations over Guangdong in winter.

The changes in ship emissions during early 2020 resulted in enhancements of simulated MDA8 ozone concentrations in the PRD and western Guangdong regions. Specifically, there were increases of 4.0 $\mu g\ m^{-3}$ (4.9%), 3.0 $\mu g\ m^{-3}$ (3.8%), and 3.4 $\mu g\ m^{-3}$ (4.2%) during the three periods of early 2020, respectively (Figure 3). Aside from these areas, the impacts of ship emissions on simulated surface ozone were mostly offshore. The changes in total anthropogenic emissions in early 2020 led to 1 to 15% increases (25th to 75th percentiles) in surface daily MDA8 ozone concentrations in the four largest PRD cities and the coastal cities in western PRD, while causing small ozone decreases (on average < 5%) over the other Guangdong cities (Figure 4). Our study found that the increased surface ozone in the four most populated PRD cities was mostly due to the decreases in land-borne anthropogenic emissions. However, over the three coastal cities in western PRD (Jiangmen, Zhongshan, and Zhuhai), changes in ship NO_x emissions led to 2 to 15% increases in daily MDA8 ozone during P2 and P3 relative to normal concentrations (Figure 4c). These cities already experience air quality nonattainment due to surface ozone, and our findings suggest that future reductions of NO_x emissions from ships could further compromise air quality in these areas.

The switch to LSFO outside the CDECA led to the simulated surface SO_2 and $PM_{2.5}$ concentrations to drop sharply over the Taiwan Strait in early 2020 (14 to 22% for SO_2 and 3.3 to 7.1% for $PM_{2.5}$, Figure 3). However, the air quality impact of that fuel switch outside the CDECA was diminished inside the CDECA and over the PRD area (Figure 3). Consequently, although it was uncertain how well the IMO's LSFO policy was enforced in early 2020, this uncertainty was unlikely to have a large impact on PRD air quality, especially in winter.

Within the CDECA, subdued ship activities caused 2.7 to 4.3% reductions of simulated SO_2 and 1.7 to 3.1% reductions of simulated $PM_{2.5}$ concentrations during three periods, respectively (Figure 3). Figure S7 quantifies the simulated responses of daily mean SO_2 and $PM_{2.5}$ concentrations in 21 Guangdong cities due to changes in ship emissions and total anthropogenic emissions, respectively. In cities along the waterways and coastal areas, ship emission changes may be responsible for as much as 10% of the simulated total reduction of surface SO_2 and $PM_{2.5}$ concentrations in early 2020. On average, the 20% (within CDECA) to 71% (domain of Figure 1) reduction of ship SO_2 emissions led to a 2.8% decrease in the simulated surface SO_2 concentrations in Guangdong cities. We thus estimated that ship emissions contributed 4 to 14% of surface SO_2 concentrations over Guangdong cities in winter. Similarly, the 20% (within CDECA) to 57% (domain of Figure 1) reduction of ship primary $PM_{2.5}$ emissions led to a 4.3% decrease in the simulated surface primary $PM_{2.5}$ concentrations in Guangdong cities. Thus, ship emissions contributed an estimated 7.5 to 22% of surface primary $PM_{2.5}$ concentrations over Guangdong cities in winter.

Liu et al.[26] previously simulated the impacts on air quality in seven coastal Guangdong cities (Zhuhai, Shenzhen, Zhongshan, Dongguan, Guangzhou in the PRD area, and Shanwei and Lufeng along the eastern Guangdong coast) due to the switch from high-sulfur content (2.43%) fuel oil to LSFO within the CDECA. They found that the switch to LSFO would lower the average surface SO_2 and $PM_{2.5}$ concentrations in these seven Guangdong cities by 30 and 6%, respectively, based on emission levels prior to the year 2015.[26] Under present-day conditions, we estimated that ship emissions contributed 4.4 to 16 and 8.8 to 25% of the ambient surface SO_2 and primary $PM_{2.5}$ concentrations, respectively, in these seven cities. Our finding, compared to Liu et al.'s[26] previous assessment in a background of much stronger land-borne pollutant emissions, indicated that the enforcement of LSFO use within the CDECA since 2019 has effectively reduced the absolute impact of ship emissions on SO_2 and $PM_{2.5}$ pollution over Southern China, at least in winter. In summer, when the prevailing southerly winds would transport marine pollutants onshore more effectively, ship emissions may affect the region's air quality more significantly.[31]

3.4. Implications for Future Ship Emission Control Policies to Benefit Air Quality in Southern China. Our analyses have implications for the future management of ship emissions over Southern China to improve regional air quality. Since January 1, 2022, a more stringent sulfur content cap of 0.1% has been applied to seagoing vessels operating within the CDECA waters around Hainan. The Chinese government is also considering extending the ultralow (<0.1%) sulfur fuel oil policy to seagoing vessels throughout the entire CDECA after January 1, 2025.[25] Our results indicated that a switch from LSFO to ultra sulfur fuel oil (a 5-fold reduction of sulfur content) within the entire CDECA could potentially reduce the contributions of ship emissions to surface SO_2 and primary $PM_{2.5}$ over Guangdong cities to below 4%, at least in winter. However, to control SO_2 and $PM_{2.5}$ pollution in Southern China, future efforts should focus on reducing land-based emissions of these pollutants and their precursors.

Since 2020, the Chinese government has aggressively promoted the synergistic reduction of air pollutants and greenhouse gas (GHG) emissions. The current guiding policy on ship emissions is China's 14th Five-Year (2021 to 2025) Plan for Green Transportation,[62] which targets a 7% decrease in total NO_x ship emissions and a 3.5% decrease in CO_2 ship emissions per unit freight turnover by 2025, relative to 2020 levels. To achieve these emission reduction goals, a series of infrastructures and control measures have been developed or planned in China. These include the development of shore-side electric power facilities, the use of liquefied natural gas as ship fuel, the use of zero- or low-carbon fuels (e.g., hydrogen and biofuels) for ships and ports, and the adoption of more energy-efficient technologies. The IMO has similarly been promoting the coreduction technologies of air pollutant and GHG emissions from international shipping, with a goal of a 50% reduction of the global ship emissions of GHG by 2050, relative to 2008 levels.[63,64]

We have demonstrated that ship emissions currently contributed approximately 40% of the surface NO_x concentrations over Southern China and that a 19% decrease in ship NO_x emissions would increase surface MDA8 ozone levels by 3.8 to 4.9% in cities along the Pearl River and the coast cities in winter. Although future reductions of NO_x emissions would effectively lower surface NO_2 levels, they would increase the risks of ozone pollution over Southern China, particularly over western Guangdong and the coastal cities in winter. During summer and fall, biogenic NMVOC emissions increase, and the ozone production in the minor cities shift toward a NO_x-limited regime. However, in the major cities of Southern China, ozone production is currently still in the NO_x-saturated or transitional regimes.[65−67] Therefore, future abatements of ship emissions should be implemented in synergy with reductions of land-borne anthropogenic NMVOC emissions to effectively alleviate surface ozone pollution over Southern China in all seasons.[68,73]

■ ASSOCIATED CONTENT

Supporting Information

The Supporting Information is available free of charge at https://pubs.acs.org/doi/10.1021/acs.est.3c04155.

Additional tables and figures showing emission profiles of NMVOCs from ships, monthly land-borne anthropogenic emissions over Southern China and their differences between early 2019 and early 2020, monthly container throughput in PRD ports, comparison of observed and simulated surface pollutant concentrations over Southern China, nested domains used for WRF-GC simulations, spatial distributions of ship emissions in early 2019 and early 2020, simulated and observed tropospheric NO_2 column concentrations, and simulated impacts of ship emission changes on surface pollutant concentrations in Guangdong cities (PDF)

■ AUTHOR INFORMATION

Corresponding Author

Tzung-May Fu − *Shenzhen Key Laboratory of Precision Measurement and Early Warning Technology for Urban Environmental Health Risks, School of Environmental Science and Engineering, Southern University of Science and Technology, Shenzhen 518055 Guangdong, China; Guangdong Provincial Observation and Research Station for Coastal Atmosphere and Climate of the Greater Bay Area, School of Environmental Science and Engineering and Center for Oceanic and Atmospheric Science at SUSTech (COAST), Southern University of Science and Technology, Shenzhen 518055 Guangdong, China; Shenzhen National Center for Applied Mathematics, Shenzhen 518055 Guangdong, China;* orcid.org/0000-0002-8556-7326; Phone: + 86 (755) 88018872; Email: fuzm@sustech.edu.cn

Authors

Xu Feng − *John A. Paulson School of Engineering and Applied Sciences, Harvard University, Cambridge, Massachusetts 02138, United States;* orcid.org/0000-0002-8226-9403

Yaping Ma − *National Meteorological Information Center, China Meteorological Administration, Beijing 100081, China*

Haipeng Lin − *John A. Paulson School of Engineering and Applied Sciences, Harvard University, Cambridge, Massachusetts 02138, United States*

Yan Zhang − *Shanghai Key Laboratory of Atmospheric Particle Pollution and Prevention (LAP3), National Observations and Research Station for Wetland Ecosystems of the Yangtze Estuary, Department of Environmental Science and Engineering, Fudan University, Shanghai 200433, China;* orcid.org/0000-0003-3087-326X

Xiaolin Wang − *Department of Atmospheric and Oceanic Sciences, School of Physics, Peking University, Beijing 100871, China;* orcid.org/0000-0001-6772-0350

Aoxing Zhang − *Shenzhen Key Laboratory of Precision Measurement and Early Warning Technology for Urban Environmental Health Risks, School of Environmental Science and Engineering, Southern University of Science and*

https://doi.org/10.1021/acs.est.3c04155
Environ. Sci. Technol. XXXX, XXX, XXX−XXX

Technology, Shenzhen 518055 Guangdong, China; orcid.org/0000-0002-0716-5452

Yupeng Yuan − *Shanghai Key Laboratory of Atmospheric Particle Pollution and Prevention (LAP3), National Observations and Research Station for Wetland Ecosystems of the Yangtze Estuary, Department of Environmental Science and Engineering, Fudan University, Shanghai 200433, China*

Zimin Han − *Shanghai Key Laboratory of Atmospheric Particle Pollution and Prevention (LAP3), National Observations and Research Station for Wetland Ecosystems of the Yangtze Estuary, Department of Environmental Science and Engineering, Fudan University, Shanghai 200433, China*

Jingbo Mao − *Shanghai Key Laboratory of Atmospheric Particle Pollution and Prevention (LAP3), National Observations and Research Station for Wetland Ecosystems of the Yangtze Estuary, Department of Environmental Science and Engineering, Fudan University, Shanghai 200433, China*

Dakang Wang − *School of Geography and Remote Sensing, Guangzhou University, Guangzhou 510006 Guangdong, China*

Lei Zhu − *Shenzhen Key Laboratory of Precision Measurement and Early Warning Technology for Urban Environmental Health Risks, School of Environmental Science and Engineering, Southern University of Science and Technology, Shenzhen 518055 Guangdong, China; Guangdong Provincial Observation and Research Station for Coastal Atmosphere and Climate of the Greater Bay Area, School of Environmental Science and Engineering, Southern University of Science and Technology, Shenzhen 518055 Guangdong, China*

Yujie Wu − *School of Public and International Affairs, Princeton University, Princeton, New Jersey 08544, United States*

Ying Li − *Department of Ocean Sciences and Engineering, Southern University of Science and Technology, Shenzhen 518055 Guangdong, China; Center for Oceanic and Atmospheric Science at SUSTech (COAST), Southern University of Science and Technology, Shenzhen 518055 Guangdong, China;* orcid.org/0000-0002-2542-7460

Xin Yang − *Shenzhen Key Laboratory of Precision Measurement and Early Warning Technology for Urban Environmental Health Risks, School of Environmental Science and Engineering, Southern University of Science and Technology, Shenzhen 518055 Guangdong, China; Guangdong Provincial Observation and Research Station for Coastal Atmosphere and Climate of the Greater Bay Area, School of Environmental Science and Engineering, Southern University of Science and Technology, Shenzhen 518055 Guangdong, China;* orcid.org/0000-0002-9173-1188

Complete contact information is available at:
https://pubs.acs.org/10.1021/acs.est.3c04155

Notes

The authors declare no competing financial interest.

ACKNOWLEDGMENTS

This work was supported by the Key-Area Research and Development Program of Guangdong Province (2020B1111360001), the Shenzhen Key Laboratory of Precision Measurement and Early Warning Technology for Urban Environmental Health Risks (ZDSYS20220606100604008), the National Natural Science Foundation of China (42325504, 42077195), the Shenzhen Science and Technology Program (KQTD20210811090048025, JCYJ20220818100611024), the Guangdong Basic and Applied Basic Research Foundation (2020B1515130003), the Guangdong University Research Project Science Team (2021KCXTD004), and the Guangdong Province Major Talent Program (2019CX01S188). Computational resources were supported by the Center for Computational Science and Engineering at the Southern University of Science and Technology.

REFERENCES

(1) World Shipping Council. The top 50 container ports. https://www.worldshipping.org/top-50-ports (accessed 01 30, 2023).

(2) The World Bank. World development indicators: Transport services. http://wdi.worldbank.org/table/5.10# (accessed 06 07, 2022).

(3) Aritua, B.; Cheng, L.; van Liere, R.; de Leijer, H. Blue routes for a new era: developing inland waterways transportation in China (International development in focus), 2020. https://openknowledge.worldbank.org/handle/10986/34415 (accessed 06 07, 2022).

(4) Ministry of Agriculture and Rural Affairs of the People's Republic of China. *China Fishery Statistical Yearbook 2020*; China Agriculture Press: Beijing, 2020.

(5) Zhang, X.; Fung, J. C.; Zhang, Y.; Lau, A. K.; Leung, K. K.; Huang, W. W. Assessing $PM_{2.5}$ emissions in 2020: the impacts of integrated emission control policies in China. *Environ. Pollut.* **2020**, *263*, 114575.

(6) Gan, L.; Che, W.; Zhou, M.; Zhou, C.; Zheng, Y.; Zhang, L.; Rangel-Buitrago, N.; Song, L. Ship exhaust emission estimation and analysis using Automatic Identification System data: The west area of Shenzhen port, China, as a case study. *Ocean Coast. Manag.* **2022**, *226*, 106245.

(7) Zhou, L.; Li, M.; Cheng, C.; Zhou, Z.; Nian, H.; Tang, R.; Chan, C. K. Real-time chemical characterization of single ambient particles at a port city in Chinese domestic emission control area—Impacts of ship emissions on urban air quality. *Sci. Total Environ.* **2022**, *819*, 153117.

(8) Air Science Group Environmental Protection Department of Hong Kong Special Administrative Region. Hong Kong emission inventory report, 2019. https://www.epd.gov.hk/epd/english/environmentinhk/air/data/emission_inve.html (accessed 12 01, 2021).

(9) Yau, P.; Lee, S.; Cheng, Y.; Huang, Y.; Lai, S.; Xu, X. Contribution of ship emissions to the fine particulate in the community near an international port in Hong Kong. *Atmos. Res.* **2013**, *124*, 61−72.

(10) Tao, J.; Zhang, L.; Cao, J.; Zhong, L.; Chen, D.; Yang, Y.; Chen, D.; Chen, L.; Zhang, Z.; Wu, Y.; Xia, Y.; Ye, S.; Zhang, R. Source apportionment of $PM_{2.5}$ at urban and suburban areas of the Pearl River Delta region, south China—With emphasis on ship emissions. *Sci. Total Environ.* **2017**, *574*, 1559−1570.

(11) Zou, B.; Huang, X.; Zhang, B.; Dai, J.; Zeng, L.; Feng, N.; He, L. Source apportionment of $PM_{2.5}$ pollution in an industrial city in southern China. *Atmos. Pollut. Res.* **2017**, *8*, 1193−1202.

(12) Zhang, R.; Zhang, Y.; Lin, H.; Feng, X.; Fu, T.-M.; Wang, Y. NO_x emission reduction and recovery during COVID-19 in East China. *Atmosphere* **2020**, *11*, 433.

(13) Zheng, B.; Zhang, Q.; Geng, G.; Chen, C.; Shi, Q.; Cui, M.; Lei, Y.; He, K. Changes in China's anthropogenic emissions and air quality during the COVID-19 pandemic in 2020. *Earth Syst. Sci. Data* **2021**, *13*, 2895−2907.

(14) Sun, W.; Zhu, L.; De Smedt, I.; Bai, B.; Pu, D.; Chen, Y.; Shu, L.; Wang, D.; Fu, T.-M.; Wang, X.; Yang, X. Global significant changes in formaldehyde (HCHO) columns observed from space at the early stage of the COVID-19 pandemic. *Geophys. Res. Lett.* **2021**, *48*, 2e020GL091265.

(15) Li, L.; Li, Q.; Huang, L.; Wang, Q.; Zhu, A.; Xu, J.; Liu, Z.; Li, H.; Shi, L.; Li, R.; Azari, M.; Wang, Y.; Zhang, X.; Liu, Z.; Zhu, Y.; Zhang, K.; Xue, S.; Ooi, M. C. G.; Zhang, D.; Chan, A. Air quality changes during the COVID-19 lockdown over the Yangtze River Delta Region: An insight into the impact of human activity pattern changes on air pollution variation. *Sci. Total Environ.* **2020**, *732*, 139282.

(16) Shi, X.; Brasseur, G. P. The response in air quality to the reduction of Chinese economic activities during the COVID-19 outbreak. *Geophys. Res. Lett.* **2020**, *47*, No. e2020GL088070.

(17) He, G.; Pan, Y.; Tanaka, T. The short-term impacts of COVID-19 lockdown on urban air pollution in China. *Nat. Sustain.* **2020**, *3*, 1005−1011.

(18) Chen, Q.; Huang, C.; Yuan, Y.; Tan, H. Influence of COVID-19 event on air quality and their association in mainland China. *Aerosol Air Qual. Res.* **2020**, *20*, 1541−1551.

(19) Lian, X.; Huang, J.; Huang, R.; Liu, C.; Wang, L.; Zhang, T. Impact of city lockdown on the air quality of COVID-19-hit of Wuhan city. *Sci. Total Environ.* **2020**, *742*, 140556.

(20) Shi, K.; Weng, J. Impacts of the COVID-19 epidemic on merchant ship activity and pollution emissions in Shanghai port waters. *Sci. Total Environ.* **2021**, *790*, 148198.

(21) Ding, J.; van der A, R. J.; Eskes, H. J.; Mijling, B.; Stavrakou, T.; van Geffen, J. H. G. M.; Veefkind, J. P. NO_x emissions reduction and rebound in China due to the COVID-19 crisis. *Geophys. Res. Lett.* **2020**, *47*, No. e2020GL089912.

(22) International Maritime Organization. IMO 2020—Cutting sulphur oxide emissions. https://www.imo.org/en/MediaCentre/HotTopics/Pages/Sulphur-2020.aspx (accessed 03 30, 2023).

(23) Fan, Q.; Zhang, Y.; Ma, W.; Ma, H.; Feng, J.; Yu, Q.; Yang, X.; Ng, S. K. W.; Fu, Q.; Chen, L. Spatial and seasonal dynamics of ship emissions over the Yangtze River Delta and East China Sea and their potential environmental influence. *Environ. Sci. Technol.* **2016**, *50*, 1322−1329.

(24) Goldsworthy, L.; Goldsworthy, B. Modelling of ship engine exhaust emissions in ports and extensive coastal waters based on terrestrial AIS data − An Australian case study. *Environ. Model. Softw.* **2015**, *63*, 45−60.

(25) Ministry of Transport of the People's Republic of China. Implementation scheme of the domestic emission control areas for atmospheric pollution from vessels, 2018. https://www.msa.gov.cn/public/documents/document/mte1/odi2~\simedisp/20190124115826051.pdf (accessed 12 01, 2021).

(26) Liu, H.; Jin, X.; Wu, L.; Wang, X.; Fu, M.; Lv, Z.; Morawska, L.; Huang, F.; He, K. The impact of marine shipping and its DECA control on air quality in the Pearl River Delta, China. *Sci. Total Environ.* **2018**, *625*, 1476−1485.

(27) Chen, D.; Zhang, Y.; Lang, J.; Zhou, Y.; Li, Y.; Guo, X.; Wang, W.; Liu, B. Evaluation of different control measures in 2014 to mitigate the impact of ship emissions on air quality in the Pearl River Delta, China. *Atmos. Environ.* **2019**, *216*, 116911.

(28) Yuan, Y.; Zhang, Y.; Mao, J.; Yu, G.; Xu, K.; Zhao, J.; Qian, H.; Wu, L.; Yang, X.; Chen, Y.; Ma, W. Diverse changes in shipping emissions around the Western Pacific ports under the coeffect of the epidemic and fuel oil policy. *Sci. Total Environ.* **2023**, *879*, 162892.

(29) International Maritime Organization *Safety of Life at Sea (SOLAS) Agreement, Regulation 19*, 2002; Chapter V, 1974, 2002 Amendments.

(30) International Maritime Organization Marine Environmental Protection Committee. Air pollution and energy efficiency sulphur monitoring programme for 2017, 2018. https://www.imokorea.org/fileup/MEPC%2072-5-3%20-%20Sulphur%20monitoring%20programme%20for%202017%20(Secretariat).pdf (accessed 2023 03 30).

(31) Zhai, J.; Yu, G.; Zhang, J.; Shi, S.; Yuan, Y.; Jiang, S.; Xing, C.; Cai, B.; Zeng, Y.; Wang, Y.; Zhang, A.; Zhang, Y.; Fu, T.-M.; Zhu, L.; Shen, H.; Ye, J.; Wang, C.; Tao, S.; Li, M.; Zhang, Y.; Yang, X. Impact of Ship Emissions on Air Quality in the Greater Bay Area in China under the Latest Global Marine Fuel Regulation. *Environ. Sci. Technol.* **2023**, *57*, 12341−12350.

(32) International Maritime Organization. Reduced limit on sulphur in marine fuel oil implemented smoothly through 2020. https://www.imo.org/en/MediaCentre/PressBriefings/pages/02-IMO-2020.aspx (accessed 2023 05 10).

(33) Zhang, Y.; Deng, F.; Man, H.; Fu, M.; Lv, Z.; Xiao, Q.; Jin, X.; Liu, S.; He, K.; Liu, H. Compliance and port air quality features with respect to ship fuel switching regulation: a field observation campaign, SEISO-Bohai. *Atmos. Chem. Phys.* **2019**, *19*, 4899−4916.

(34) Zhang, X.; Zhang, Y.; Liu, Y.; Zhao, J.; Zhou, Y.; Wang, X.; Yang, X.; Zou, Z.; Zhang, C.; Fu, Q.; Xu, J.; Gao, W.; Li, N.; Chen, J. Changes in the SO_2 Level and $PM_{2.5}$ Components in Shanghai Driven by Implementing the Ship Emission Control Policy. *Environ. Sci. Technol.* **2019**, *53*, 11580−11587.

(35) Li, M.; Zhang, Q.; Zheng, B.; Tong, D.; Lei, Y.; Liu, F.; Hong, C.; Kang, S.; Yan, L.; Zhang, Y.; Bo, Y.; Su, H.; Cheng, Y.; He, K. Persistent growth of anthropogenic non-methane volatile organic compound (NMVOC) emissions in China during 1990−2017: drivers, speciation and ozone formation potential. *Atmos. Chem. Phys.* **2019**, *19*, 8897−8913.

(36) Li, M.; Zhang, Q.; Streets, D. G.; He, K. B.; Cheng, Y. F.; Emmons, L. K.; Huo, H.; Kang, S. C.; Lu, Z.; Shao, M.; Su, H.; Yu, X.; Zhang, Y. Mapping Asian anthropogenic emissions of non-methane volatile organic compounds to multiple chemical mechanisms. *Atmos. Chem. Phys.* **2014**, *14*, 5617−5638.

(37) Zheng, B.; Tong, D.; Li, M.; Liu, F.; Hong, C.; Geng, G.; Li, H.; Li, X.; Peng, L.; Qi, J.; Yan, L.; Zhang, Y.; Zhao, H.; Zheng, Y.; He, K.; Zhang, Q. Trends in China's anthropogenic emissions since 2010 as the consequence of clean air actions. *Atmos. Chem. Phys.* **2018**, *18*, 14095−14111.

(38) Lin, H.; Feng, X.; Fu, T.-M.; Tian, H.; Ma, Y.; Zhang, L.; Jacob, D. J.; Yantosca, R. M.; Sulprizio, M. P.; Lundgren, E. W.; Zhuang, J.; Zhang, Q.; Lu, X.; Zhang, L.; Shen, L.; Guo, J.; Eastham, S. D.; Keller, C. A. WRF-GC (v1.0): online coupling of WRF (v3.9.1.1) and GEOS-Chem (v12.2.1) for regional atmospheric chemistry modeling − Part 1: Description of the one-way model. *Geosci. Model Dev.* **2020**, *13*, 3241−3265.

(39) Feng, X.; Lin, H.; Fu, T.-M.; Sulprizio, M. P.; Zhuang, J.; Jacob, D. J.; Tian, H.; Ma, Y.; Zhang, L.; Wang, X.; Chen, Q.; Han, Z. WRF-GC (v2.0): online two-way coupling of WRF (v3.9.1.1) and GEOS-Chem (v12.7.2) for modeling regional atmospheric chemistry−meteorology interactions. *Geosci. Model Dev.* **2021**, *14*, 3741−3768.

(40) Lin, H.; Jacob, D. J.; Lundgren, E. W.; Sulprizio, M. P.; Keller, C. A.; Fritz, T. M.; Eastham, S. D.; Emmons, L. K.; Campbell, P. C.; Baker, B.; Saylor, R. D.; Montuoro, R. Harmonized Emissions Component (HEMCO) 3.0 as a versatile emissions component for atmospheric models: application in the GEOS-Chem, NASA GEOS, WRF-GC, CESM2, NOAA GEFS-Aerosol, and NOAA UFS models. *Geosci. Model Dev.* **2021**, *14*, 5487−5506.

(41) Skamarock, W. C.; Klemp, J. B.; Dudhia, J.; Gill, D. O.; Barker, D. M.; Duda, M. G.; Huang, X.; Wang, W.; Powers, J. G. *NCAR Tech. Note NCAR/TN-475+STR: A Description of the Advanced Research WRF Model Version 3*; National Center for Atmospheric Research, 2008.

(42) Skamarock, W. C.; Klemp, J. B.; Dudhia, J.; Gill, D. O.; Liu, Z.; Berner, J.; Huang, X. *NCAR Tech. Note NCAR/TN-556+STR: A Description of the Advanced Research WRF Model Version 4*; The Tech Report, 2019.

(43) Bey, I.; Jacob, D. J.; Yantosca, R. M.; Logan, J. A.; Field, B. D.; Fiore, A. M.; Li, Q.; Liu, H. Y.; Mickley, L. J.; Schultz, M. G. Global modeling of tropospheric chemistry with assimilated meteorology: Model description and evaluation. *J. Geophys. Res. Atmos.* **2001**, *106*, 23073−23095.

(44) Bates, K. H.; Jacob, D. J. A new model mechanism for atmospheric oxidation of isoprene: global effects on oxidants, nitrogen oxides, organic products, and secondary organic aerosol. *Atmos. Chem. Phys.* **2019**, *19*, 9613−9640.

https://doi.org/10.1021/acs.est.3c04155
Environ. Sci. Technol. XXXX, XXX, XXX−XXX

(45) Holmes, C. D.; Bertram, T. H.; Confer, K. L.; Graham, K. A.; Ronan, A. C.; Wirks, C. K.; Shah, V. The role of clouds in the tropospheric NO_x cycle: A new modeling approach for cloud chemistry and its global implications. *Geophys. Res. Lett.* **2019**, *46*, 4980−4990.

(46) Wang, X.; Jacob, D. J.; Downs, W.; Zhai, S.; Zhu, L.; Shah, V.; Holmes, C. D.; Sherwen, T.; Alexander, B.; Evans, M. J.; Eastham, S. D.; Neuman, J. A.; Veres, P. R.; Koenig, T. K.; Volkamer, R.; Huey, L. G.; Bannan, T. J.; Percival, C. J.; Lee, B. H.; Thornton, J. A. Global tropospheric halogen (Cl, Br, I) chemistry and its impact on oxidants. *Atmos. Chem. Phys.* **2021**, *21*, 13973−13996.

(47) National Centers for Environmental Prediction. *NCEP FNL Operational Model Global Tropospheric Analyses, Continuing from July 1999, Research Data Archive at the National Center for Atmospheric Research*; Computational and Information Systems Laboratory, 2000.

(48) Jiang, Z.; Jolleys, M. D.; Fu, T.-M.; Palmer, P. I.; Ma, Y. P.; Tian, H.; Li, J.; Yang, X. Spatiotemporal and probability variations of surface $PM_{2.5}$ over China between 2013 and 2019 and the associated changes in health risks: An integrative observation and model analysis. *Sci. Total Environ.* **2020**, *723*, 137896.

(49) Wang, X.; Fu, T.-M.; Zhang, L.; Cao, H.; Zhang, Q.; Ma, H.; Shen, L.; Evans, M. J.; Ivatt, P. D.; Lu, X.; Chen, Y.; Zhang, L.; Feng, X.; Yang, X.; Zhu, L.; Henze, D. K. Sensitivities of ozone air pollution in the Beijing−Tianjin−Hebei area to local and upwind precursor emissions using adjoint modeling. *Environ. Sci. Technol.* **2021**, *55*, 5752−5762.

(50) van Geffen, J.; Boersma, K. F.; Eskes, H.; Sneep, M.; ter Linden, M.; Zara, M.; Veefkind, J. P. S5P TROPOMI NO_2 slant column retrieval: method, stability, uncertainties and comparisons with OMI. *Atmos. Meas. Technol.* **2020**, *13*, 1315−1335.

(51) Veefkind, J.; Aben, I.; McMullan, K.; Förster, H.; de Vries, J.; Otter, G.; Claas, J.; Eskes, H.; de Haan, J.; Kleipool, Q.; van Weele, M.; Hasekamp, O.; Hoogeveen, R.; Landgraf, J.; Snel, R.; Tol, P.; Ingmann, P.; Voors, R.; Kruizinga, B.; Vink, R.; Visser, H.; Levelt, P. TROPOMI on the ESA Sentinel-5 Precursor: A GMES mission for global observations of the atmospheric composition for climate, air quality and ozone layer applications. *Remote Sens. Environ.* **2012**, *120*, 70−83.

(52) European Space Agency's (ESA) and Koninklijk Nederlands Meteorologisch Instituut (KNMI). *Sentinel-5P TROPOMI Tropospheric NO2 1-Orbit L2 5.5km x 3.5km*; Goddard Earth Sciences Data and Information Services Center (GES DISC), 2021.

(53) Zhu, L.; Jacob, D. J.; Mickley, L. J.; Marais, E. A.; Cohan, D. S.; Yoshida, Y.; Duncan, B. N.; González Abad, G.; Chance, K. V. Anthropogenic emissions of highly reactive volatile organic compounds in eastern Texas inferred from oversampling of satellite (OMI) measurements of HCHO columns. *Environ. Res. Lett.* **2014**, *9*, 114004.

(54) Zhu, L.; Mickley, L. J.; Jacob, D. J.; Marais, E. A.; Sheng, J.; Hu, L.; Abad, G. G.; Chance, K. Long-term (2005−2014) trends in formaldehyde (HCHO) columns across North America as seen by the OMI satellite instrument: Evidence of changing emissions of volatile organic compounds. *Geophys. Res. Lett.* **2017**, *44*, 7079−7086.

(55) Platt, U.; Stutz, J. *Differential Optical Absorption Spectroscopy: Principles and Applications*; Springer Berlin Heidelberg, 2008; pp 135−174.

(56) Ministry of Transport of the People's Republic of China. Monthly statistical report on the throughputs of cargo and containers in Chinese ports for January and February of 2019 and 2020. 2019−2020. https://www.mot.gov.cn/tongjishuju/gangkouhuowulvkettl/index_1.html (accessed 06 30, 2022).

(57) Shenzhen Bureau of Transportation. Monthly statistical report on transport operation indicators for January and February of 2019 and 2020. 2019−2020. http://jtys.sz.gov.cn/gkmlpt/index#1466 (accessed 06 30, 2022).

(58) Hong Kong Maritime and Port Board. Container throughputs of Hong Kong port and Kwai Tsing container terminals (monthly), 2022. https://www.hkmpb.gov.hk/document/HKP_KTCT-stat.pdf. (accessed 06 30, 2022).

(59) Wang, S.; Zhang, Y.; Ma, J.; Zhu, S.; Shen, J.; Wang, P.; Zhang, H. Responses of decline in air pollution and recovery associated with COVID-19 lockdown in the Pearl River Delta. *Sci. Total Environ.* **2021**, *756*, 143868.

(60) Pei, C.; Yang, W.; Zhang, Y.; Song, W.; Xiao, S.; Wang, J.; Zhang, J.; Zhang, T.; Chen, D.; Wang, Y.; Chen, Y.; Wang, X. Decrease in ambient volatile organic compounds during the COVID-19 lockdown period in the Pearl River Delta region, south China. *Sci. Total Environ.* **2022**, *823*, 153720.

(61) Statistics Bureau of Guangdong Province. Bulletin of the seventh National Census of Guangdong Province, 2021. http://stats.gd.gov.cn/attachment/0/421/421309/3283428.pdf (accessed 06 30, 2022).

(62) Ministry of Transport of the People's Republic of China. China's 14th Five-Year (2021 to 2025) Plan of green transportation, 2021. http://www.gov.cn/zhengce/zhengceku/2022-01/21/content_5669662.htm (accessed 06 30, 2022).

(63) International Maritime Organization. Nitrogen Oxides (NOx)—Regulation 13. https://www.imo.org/en/OurWork/Environment/Pages/Nitrogen-oxides-(NOx)-%E2%80%93-Regulation-13.aspx (accessed 04 30, 2023).

(64) International Maritime Organization Marine Environmental Protection Committee. Adoption of the initial IMO strategy on reduction of GHG Emissions from ships and existing IMO activity related to reducing GHG emissions in the shipping sector, 2018. https://unfccc.int/sites/default/files/resource/250_IMO%20submission_Talanoa%20Dialogue_April%202018.pdf (accessed 04 30, 2023).

(65) Shao, M.; Zhang, Y.; Zeng, L.; Tang, X.; Zhang, J.; Zhong, L.; Wang, B. Ground-level ozone in the Pearl River Delta and the roles of VOC and NO_x in its production. *J. Environ. Manage.* **2009**, *90*, 512−518.

(66) Ou, J.; Yuan, Z.; Zheng, J.; Huang, Z.; Shao, M.; Li, Z.; Huang, X.; Guo, H.; Louie, P. K. K. Ambient Ozone Control in a Photochemically Active Region: Short-Term Despiking or Long-Term Attainment? *Environ. Sci. Technol.* **2016**, *50*, 5720−5728.

(67) Yu, D.; Tan, Z.; Lu, K.; Ma, X.; Li, X.; Chen, S.; Zhu, B.; Lin, L.; Li, Y.; Qiu, P.; Yang, X.; Liu, Y.; Wang, H.; He, L.; Huang, X.; Zhang, Y. An explicit study of local ozone budget and NOx-VOCs sensitivity in Shenzhen China. *Atmos. Environ.* **2020**, *224*, 117304.

(68) Morrison, H.; Thompson, G.; Tatarskii, V. Impact of Cloud Microphysics on the Development of Trailing Stratiform Precipitation in a Simulated Squall Line: Comparison of One- and Two-Moment Schemes. *Mon. Weather Rev.* **2009**, *137*, 991−1007.

(69) Iacono, M. J.; Delamere, J. S.; Mlawer, E. J.; Shephard, M. W.; Clough, S. A.; Collins, W. D. Radiative forcing by long-lived greenhouse gases: Calculations with the AER radiative transfer models. *J. Geophys. Res. Atmos.* **2008**, *113*, D13103.

(70) Nakanishi, M.; Niino, H. An improved mellor-yamada level-3 model: Its numerical stability and application to a regional prediction of advection fog. *Bound.-Lay. Meteorol.* **2006**, *119*, 397−407.

(71) Chen, F.; Dudhia, J. Coupling an advanced land surface-hydrology model with the Penn State-NCAR MM5 modeling system. Part I: Model implementation and sensitivity. *Mon. Weather Rev.* **2001**, *129*, 569−585.

(72) Chen, F.; Dudhia, J. Coupling an advanced land surface-hydrology model with the Penn State-NCAR MM5 modeling system. Part II: Preliminary model validation. *Mon. Weather Rev.* **2001**, *129*, 587−604.

(73) Jimenez, P. A.; Dudhia, J.; Gonzalez-Rouco, J. F.; Navarro, J.; Montavez, J. P.; Garcia-Bustamante, E. A Revised Scheme for the WRF Surface Layer Formulation. *Mon. Weather Rev.* **2012**, *140*, 898−918.

(74) Tiedtke, M. A comprehensive mass flux scheme for cumulus parameterization in large-scale models. *Mon. Weather. Rev.* **1989**, *117*, 1779−1800.

(75) Zhang, C.; Wang, Y.; Hamilton, K. Improved representation of boundary layer clouds over the southeast Pacific in ARW-WRF using

https://doi.org/10.1021/acs.est.3c04155
Environ. Sci. Technol. XXXX, XXX, XXX−XXX

a modified Tiedtke cumulus parameterization scheme. *Mon. Weather Rev.* **2011**, *139*, 3489−3513.
(76) Zhang, C.; Wang, Y. Projected future changes of tropical cyclone activity over the western North and South Pacific in a 20-km-Mesh regional climate model. *J. Clim.* **2017**, *30*, 5923−5941.